Enhanced selectivity of CO_2 over CH_4 in sulphonate-, carboxylate- and iodo-functionalized UiO-66 frameworks†

Shyam Biswas,[a] Jian Zhang,[b] Zhibao Li,[b] Ying-Ya Liu,[a] Maciej Grzywa,[c] Lixian Sun,[b,d] Dirk Volkmer[c] and Pascal Van Der Voort*[a]

Three new functionalized UiO-66-X (X = –SO_3H, **1**; –CO_2H, **2**; –I; **3**) frameworks incorporating BDC-X (BDC: 1,4-benzenedicarboxylate) linkers have been synthesized by a solvothermal method using conventional electric heating. The as-synthesized (AS) as well as the thermally activated compounds were characterized by X-ray powder diffraction (XRPD), diffuse reflectance infrared Fourier transform (DRIFT) spectroscopy, thermogravimetric (TG), and elemental analysis. The occluded H_2BDC-X molecules can be removed by exchange with polar solvent molecules followed by thermal treatment under vacuum leading to the empty-pore forms of the title compounds. Thermogravimetric analysis (TGA) and temperature-dependent XRPD (TDXRPD) experiments indicate that **1**, **2** and **3** are stable up to 260, 340 and 360 °C, respectively. The compounds maintain their structural integrity in water, acetic acid and 1 M HCl, as verified by XRPD analysis of the samples recovered after suspending them in the respective liquids. As confirmed by N_2, CO_2 and CH_4 sorption analyses, all of the thermally activated compounds exhibit significant microporosity ($S_{Langmuir}$: 769–842 $m^2\ g^{-1}$), which are comparable to that of the parent UiO-66 compound. Compared to the unfunctionalized UiO-66 compound, all the three functionalized solids possess higher ideal selectivity in adsorption of CO_2 over CH_4 at 33 °C.

Introduction

Next to conventional industrial adsorbents like zeolites, mesoporous silicas and active carbons, the design and development of new CO_2 capture materials is still relevant to improve the adsorption capacity and selectivity or regeneration ability.[1] Metal–organic frameworks (MOFs)[2–4] are a relatively new class of highly crystalline and nanoporous materials that have been the subject of tremendous research interest over the past few years due to their potential applications in a wide range of areas such as gas storage/separation,[5–7] catalysis[8,9] and drug delivery.[10–13] Built up from inorganic building units and polytopic organic linkers, the modular character of MOFs allows the systematic tuning of the pore features (dimensions or surface property) by attaching functional groups (having different dimensions, polarities, hydrophilicities, acidities, *etc.*) to the organic linker, without altering the underlying topology of the framework. The functionalization of MOFs has been shown to affect their sorption[14–18] and selectivity[19,20] as well as thermal and chemical stability.[21]

MOFs might be a potential alternative to zeolites and active carbons in adsorption technologies. Owing to their many fascinating features, MOFs have shown promising performances over conventional adsorbents in separation of gas mixtures.[7,22–26] Both experiments[27] and computational methods[28,29] have demonstrated that the introduction of polar functional groups in the frameworks significantly enhances the CO_2 adsorption capacity of MOFs. Moreover, MOFs with coordinatively unsaturated metal sites have been shown to adsorb increased amounts of CO_2.[30] However, some of the famous MOFs[31–35] that have shown potential for adsorption/separation suffer from low physicochemical stabilities (moisture, thermal or acid–base) and thus are not suitable for industrial applications.

[a]*Department of Inorganic and Physical Chemistry, Centre for Ordered Materials, Organometallics and Catalysis, Ghent University, Krijgslaan 281-S3, 9000 Ghent, Belgium. E-mail: pascal.vandervoort@ugent.be; Fax: +32 9 264 49 83; Tel: +32 964 44 42*

[b]*Materials and Thermochemistry Laboratory, Dalian Institute of Chemical Physics, Chinese Academy of Sciences, Dalian, 116023, China*

[c]*Institute of Physics, Chair of Solid State and Material Science, Augsburg University, Universitätsstrasse 1, 86135 Augsburg, Germany*

[d]*Guangxi Key Laboratory of Information Materials, Guilin University of Electronic Technology, Guilin 541004, China*

†Electronic supplementary information (ESI) available: Additional ambient and temperature-dependent XRPD patterns, DRIFT spectra, TG curves, tables containing results of TG, DRIFT and elemental analyses. See DOI: 10.1039/c3dt32288b

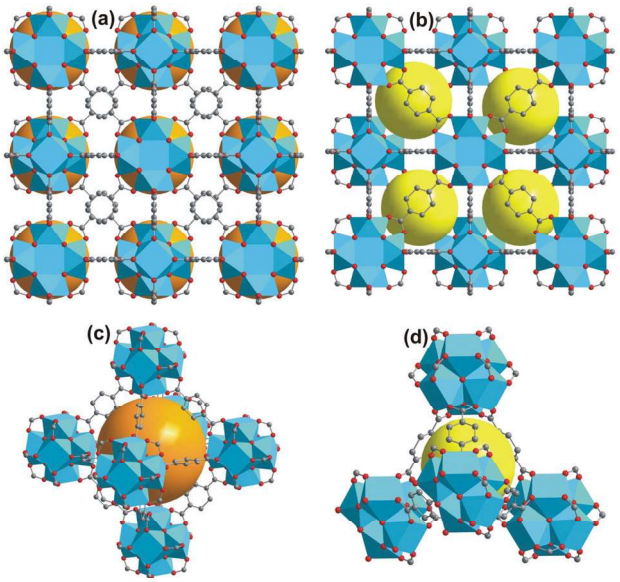

Fig. 1 Ball-and-stick representations of the 3D cubic framework structure of UiO-66. (a, b) Parts of the framework showing spatial arrangements of the octahedral and the tetrahedral cages, represented by orange and yellow spheres, respectively. (c, d) Magnified views of the octahedral and the tetrahedral cages. Zr atoms are displayed as octahedra (color codes: Zr, blue; C, gray; O, red). The hydrogen atoms and guest molecules have been removed from all structural plots for clarity. The figure was drawn using atomic coordinates provided in ref. 67.

The Zr-based MOF UiO-66[36] (UiO: University of Oslo) has attracted immense interest recently due to its high thermal and chemical stability as well as promising properties for CO_2/CH_4 gas separation including good selectivity, high working capacity and low cost regenerability.[37,38] Its cubic 3D framework consists of a centric octahedral cage connected to eight corner tetrahedral cages through triangular windows (Fig. 1). The possibility of functionalization of the UiO-66 framework has been successfully demonstrated without altering the physicochemical properties of the parent material.[21,39–46] Especially, the amino- and the dimethyl-functionalized UiO-66 solids have shown improved CO_2 uptakes over the unfunctionalized material.[39,47] In an elaborate computational study,[47] the effect of organic functionalization on the CO_2/CH_4 adsorption selectivity has been explored. The simulations suggested that the attachment of polar functional groups such as $-SO_3H$ and $-CO_2H$ to the UiO-66 framework would lead to improvement of both CO_2 adsorption capacity and CO_2/CH_4 separation performance. Very recently, the UiO-66-SO_3H compound has been reported[44] to be unstable upon guest removal. In the same report, a mixed-linker UiO-66 compound incorporating both BDC (BDC: 1,4-benzenedicarboxylate) and BDC-SO_3H has been prepared. The mixed-linker UiO-66 compound showed enhanced stability and improved heat of adsorption for CO_2 compared to the parent UiO-66. In this article, we wish to report on the stable version of the UiO-66-SO_3H compound, which has been synthesized by a modification of the literature route.[44] In addition, the carboxylate- and the iodo-functionalized UiO-66 compounds have been prepared. The thermal and chemical stability as well as the CO_2/CH_4 adsorption selectivity of the three functionalized UiO-66-X (X = $-SO_3H$, **1**; $-CO_2H$, **2**; –I; **3**) (Scheme 1) compounds are discussed.

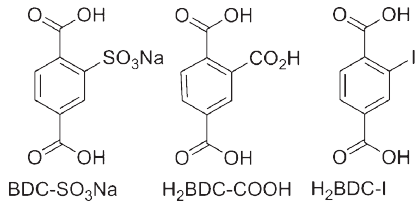

Scheme 1 Functionalized terephthalate linker molecules BDC-X used for synthesizing UiO-66-X compounds.

Experimental

Materials and general methods

The H_2BDC-I ligand was synthesized as described previously.[48] All other starting materials were of reagent grade and used as received from the commercial supplier. Diffuse-reflectance infrared Fourier transform (DRIFT) spectra were recorded with a Thermo Nicolet 6700 FTIR spectrometer equipped with a nitrogen-cooled MCT detector and a KBr beam splitter. The DRIFT cell was connected to a vacuum manifold. The following indications are used to characterize absorption bands: very strong (vs), strong (s), medium (m), weak (w), shoulder (sh), and broad (br). Elemental analyses (C, H, N) were carried out with a Thermo Scientific Flash 2000 CHNS-O analyzer equipped with a TCD detector. Thermogravimetric analysis (TGA) was performed with a Netzsch STA-409CD thermal analyzer in a temperature range of 25–600 °C under an air atmosphere at a heating rate of 2 °C min^{-1}. Ambient temperature X-ray powder diffraction (XRPD) patterns were recorded with a Thermo Scientific ARL X'Tra diffractometer operated at 40 kV, 40 mA with Cu-Kα (λ = 1.5406 Å) radiation. Le Bail fits were performed by using the Jana2006 program.[49] Temperature-dependent XRPD patterns were collected with a Bruker D8 Discover X-ray diffractometer equipped with a Vantec position sensitive detector (PSD); the XRD patterns were recorded from room temperature to 500 (**3**), 700 (**1**) or 800 (**2**) °C with a temperature ramp of 0.1 °C s^{-1} in air flow. Energy-dispersive X-ray (EDX) analysis was performed with a FEI Quanta 200FEG environmental scanning electron microscope equipped with an EDX detector. The accelerating voltage used in the EDX measurement was 20 kV. The solution ^{1}H-NMR spectra were recorded on a Bruker AM 300 spectrometer at 300 MHz. The compounds were digested in 570 μL of d_6-DMSO and 30 μL of 48% HF (caution!) before the NMR measurements. The N_2 sorption isotherms up to 1 bar were measured by using a Belsorp Mini apparatus at −196 °C. The high-pressure CO_2 and CH_4 sorption isotherms were recorded with a commercial pressure composition isotherm (PCI) unit provided by Advanced Materials Co. (USA) at 33 °C. The methanol-exchanged form of the

compounds was heated at 65 °C for 24 h under dynamic vacuum prior to the sorption experiments.

Syntheses

UiO-66 was synthesized and activated according to a literature method.[50] The usual characterization experiments (XRPD, TGA, IR spectroscopy, and sorption analysis) were performed to confirm its purity.

$[Zr_6O_4(OH)_4(BDC\text{-}SO_3H)_6]\cdot 1.5(H_2BDC\text{-}SO_3H)$ (UiO-66-SO_3H-AS) (1-AS). A mixture of $ZrOCl_2\cdot 8H_2O$ (100 mg, 0.31 mmol), BDC-SO_3Na (83 mg, 0.31 mmol) and formic acid (1.17 mL, 31.03 mmol) in 3 mL of *N*,*N*′-dimethylacetamide (DMA) was placed in a glass tube (10 mL). The tube was sealed and heated in a programmable heating block to 150 °C at a rate of 2.2 °C min^{-1}, held at this temperature for 24 h, then cooled to room temperature at a rate of 2.2 °C min^{-1}. The colorless precipitate was collected by filtration, and dried in air. The yield was 110 mg (0.04 mmol, 85%). DRIFT (KBr, cm^{-1}): 3408 (br), 3068 (br), 2809 (w), 2474 (br), 1661 (s), 1592 (vs), 1494 (m), 1413 (vs), 1235 (s), 1177 (s), 1079 (s), 1027 (s), 952 (w), 871 (w), 831 (m), 779 (s), 664 (s).

$[Zr_6O_4(OH)_4(BDC\text{-}CO_2H)_6]\cdot 2.0(H_2BDC\text{-}CO_2H)$ (UiO-66-CO_2H-AS) (2-AS). A mixture of $ZrO(NO_3)_2\cdot xH_2O$ (100 mg, 0.43 mmol), H_2BDC-CO_2H (182 mg, 0.86 mmol) and benzoic acid (1.58 g, 12.94 mmol) in 3 mL of *N*,*N*′-dimethylformamide (DMF) was placed in a glass tube (10 mL). The tube was sealed and heated in a programmable heating block to 150 °C at a rate of 2.2 °C min^{-1}, held at this temperature for 24 h, then cooled to room temperature at a rate of 2.2 °C min^{-1}. The colorless precipitate was collected by filtration, and dried in air. The yield was 160 mg (0.07 mmol, 95%). DRIFT (KBr, cm^{-1}): 3068 (br), 2930 (br), 2531 (br), 1921 (w), 1719 (m), 1661 (s), 1597 (vs), 1494 (m), 1401 (vs), 1258 (m), 1177 (m), 1114 (m), 1067 (m), 1027 (w), 934 (w), 871 (w), 831 (w), 814 (w), 773 (m), 722 (m), 664 (s).

$[Zr_6O_4(OH)_4(BDC\text{-}I)_6]\cdot 2.0(H_2BDC\text{-}I)$ (UiO-66-I-AS) (3-AS). A mixture of $ZrCl_4$ (50 mg, 0.21 mmol), H_2BDC-I (63 mg, 0.21 mmol) and formic acid (0.24 mL, 6.36 mmol) in 3 mL of DMF was placed in a glass tube (10 mL). The tube was sealed and heated in a programmable heating block to 150 °C at a rate of 2.2 °C min^{-1}, held at this temperature for 24 h, then cooled to room temperature at a rate of 2.2 °C min^{-1}. The colorless precipitate was collected by filtration, and dried in air. The yield was 90 mg (0.03 mmol, 85%). DRIFT (KBr, cm^{-1}): 3051 (br), 2923 (m), 2860 (w), 2774 (br), 1661 (s), 1592 (vs), 1471 (s), 1390 (vs), 1281 (w), 1252 (w), 1154 (w), 1096 (w), 1039 (m), 923 (w), 866 (w), 825 (m), 762 (s), 722 (w), 687 (s).

Elemental analyses of the as-synthesized and the activated forms of the three UiO-66-X compounds have been summarized in Table 1.

Table 1 Elemental analyses of the as-synthesized and the thermally activated forms of the UiO-66-X compounds

Compound	$C_{obs.}/C_{cal.}$ (%)	$H_{obs.}/H_{cal.}$ (%)
1-AS	28.30/28.66	1.62/1.48
1	25.35/25.39	1.67/1.86
2-AS	36.40/36.82	1.62/1.71
2	27.63/27.90	3.06/3.12
3-AS	25.30/25.59	1.02/1.07
3	23.06/23.13	1.39/1.21

Activation of the compounds

A suspension of the AS-form of each compound amounting to 0.3 g collected from different batches was stirred in DMF (20 mL) for 12 h at ambient conditions. The filtered solid was further stirred in methanol (30 mL) for 24 h at ambient conditions. The methanol-exchanged forms of the compounds were subsequently heated at 65 °C under dynamic vacuum for 24 h to get the activated forms of the compounds.

Results and discussion

Syntheses and activation

In order to optimize the synthesis conditions of the UiO-66-X compounds, mixtures of Zr salts ($ZrCl_4$, $ZrO(NO_3)_2\cdot xH_2O$ or $ZrOCl_2\cdot 8H_2O$), BDC-X linkers and modulators/additives[51] (H_2O, conc. HCl, benzoic acid, formic acid, acetic acid or trifluoroacetic acid) in all possible combinations were heated in polar amide solvents (DMA, DMF and *N*,*N*′-diethylformamide). For the synthesis of **1** and **3**, the molar ratio between the particular Zr salt and the respective H_2BDC-X linker was 1 : 1. For the preparation of **2**, maintaining a molar ratio between the Zr salt and the linker of 1 : 2 was found to be crucial. An excess of the modulator than the required stoichiometric ratio (metal salt : modulator = 1 : 30 for **2** and **3**; 1 : 100 for **1**) was employed for all the three compounds. It is worth noting that modulators/additives have been formerly employed to synthesize various Zr-based MOFs.[39,41,44,46,50,52–64] Compound **1**, which has been synthesized recently[44] by the solvothermal reaction of $ZrCl_4$, BDC-SO_3Na and acetic acid in DMF, appeared to be unstable upon removal of guest molecules. In contrast, the reaction conditions presented here produced a highly crystalline solid that retained its crystallinity after removing the guest molecules from the pores. We attribute the difference in stability between the previously reported solid and the present one to different synthetic conditions as well as different guest molecules encapsulated within the pores. The traces of water introduced in the reaction medium through the employment of $ZrOCl_2\cdot 8H_2O$ might contribute to the formation of –OH groups that are part of the $[Zr_6O_4(OH)_4]$ structural building units (see Structure description section). Similar to the previous report,[44] the anionic BDC-SO_3Na linker becomes protonated during the synthesis in acidic medium. The absence of sodium in compound **1** has been confirmed by EDX analysis (Fig. S1, ESI†).

In order to verify that the linkers did not undergo any side reaction (*e.g.* substitution) during the solvothermal syntheses, the UiO-66-X solids were digested and solution ^{1}H-NMR spectra (Fig. S2–S4, ESI†) were measured. The similarity between the NMR spectra of the digested UiO-66-X materials and the pure linkers clearly demonstrates the structural

integrity of the pre-functionalized linkers during the solvothermal syntheses.

The AS-forms of the three compounds contain non-coordinated H_2BDC-X linker molecules encapsulated within the pores which were removed by a three-step procedure. The guest molecules were first exchanged by stirring the AS compounds with a polar solvent such as DMF. In the second step, the DMF molecules were exchanged by stirring the DMF-exchanged compounds with more volatile and thus easily removable methanol molecules. In the third step, the methanol molecules were removed from the pores by heating at a low temperature (65 °C) under dynamic vacuum for 24 h to get the thermally activated compounds. After cooling to room temperature, the thermally activated compounds adsorb water from air (denoted as "hydrated form" hereafter).

DRIFT analysis

The DRIFT spectra of the AS and thermally activated forms of each of the isostructural UiO-66-X compounds (Fig. S5 and S6, ESI†) are similar, as expected. In the DRIFT spectra of the AS forms of the three compounds, the strong absorption bands due to asymmetric and symmetric $-CO_2$ stretching vibrations of the coordinated terephthalate linker molecules are located in the regions 1593–1596 cm^{-1} and 1392–1412 cm^{-1}, respectively.[65] The additional strong absorption bands at *ca.* 1658 cm^{-1}, observed in the DRIFT spectra of the AS forms of the compounds, can be attributed to the protonated form ($-CO_2H$) of unreacted or guest BDC-X linker molecules.[65] The absorption bands of the occluded H_2BDC-X molecules are absent or significantly reduced in intensity in the DRIFT spectra of the empty-pore forms of the three compounds, suggesting almost complete activation. The strong absorption band at 1710 cm^{-1} in the DRIFT spectra of **2-AS** and **2** can be attributed to the stretching vibration of the attached $-CO_2H$ group. The stretching vibration of the μ_3-OH group exhibits medium absorption bands in the region 3673–3680 cm^{-1} in the DRIFT spectra of hydrated **1** and **3**.[36] The asymmetric and symmetric stretching vibration bands due to the attached O═S═O groups are located at 1230 and 1180 cm^{-1} in the DRIFT spectra of **1-AS** and **1**.[66]

Structure description

The refined lattice parameters (Table 2) of the thermally activated forms of the three functionalized compounds determined from their XRPD patterns collected at ambient conditions are similar to the unfunctionalized UiO-66 compound.[36] The three functionalized compounds are thus isostructural with UiO-66. Le Bail fits of the XRPD patterns of the UiO-66-X compounds are presented in Fig. S7–S9, ESI.† As described by Lillerud's group,[36] the hydroxylated form of UiO-66 is constructed from hexanuclear $[Zr_6O_4(OH)_4]$ building units in which the triangular faces of the Zr_6-octahedron are alternatively capped by μ_3-O and μ_3-OH groups. The Zr_6-polyhedra are interconnected along the edges through carboxylates of twelve BDC linkers to form a cubic, three-dimensional (3D) framework (Fig. 1a, b). Each Zr atom is coordinated with eight O atoms, forming a square-antiprismatic geometry. One square face of the square antiprism consists of O atoms from the carboxylates, whereas the second square face is built up of O atoms from the μ_3-O and μ_3-OH groups. In the resulting microporous framework, each centric octahedral cage (Fig. 1c, free diameter: ~11 Å) is linked with eight corner tetrahedral cages (Fig. 1d, free diameter: ~8 Å) through trigonal windows (~6 Å). In the AS-forms of the functionalized compounds, the cages are occupied by guest H_2BDC-X linker molecules at ambient conditions. The guest molecules are removed by a three-step activation procedure leading to the empty-pore forms of the compounds.

Table 2 Molecular formulae and refined lattice parameters for the thermally activated **1**, **2** and **3** having cubic unit cells

Compound	Molecular formula	a (Å)	V (Å^3)
1	$[Zr_6O_4(OH)_4(C_8H_4O_7S)_6]\cdot 7(H_2O)$	20.824(1)	9029.8(6)
2	$[Zr_6O_4(OH)_4(C_9H_4O_6)_6]\cdot 22(H_2O)$	20.8202(3)	9025.1(1)
3	$[Zr_6O_4(OH)_4(C_8H_3IO_4)_6]\cdot 4(H_2O)$	20.8076(5)	9008.8(2)
UiO-66[36]	$[Zr_6O_6(C_8H_4O_4)_6]$	20.7004(2)	8870.3(2)

Thermal and chemical stability

To examine the thermal stability of all the three compounds, thermogravimetric analyses (TGA) were performed on the different forms of the compounds in an air atmosphere. On the basis of the TG analyses, **1**, **2** and **3** are thermally stable up to 260, 340 and 360 °C, respectively. The thermal stabilities of **2** and **3** are comparable to that of unfunctionalized UiO-66 (430 °C). Noticeably, **1** possesses significantly lower thermal stability compared to **2** and **3**, in spite of having the same framework topology.

In the TG curves of the AS forms of the compounds (Fig. S10, ESI†), one weight loss step that occurs below the decomposition temperature of the frameworks can be assigned to the removal of the guest H_2BDC-X linker molecules. Below the decomposition temperature, the hydrated forms of all the three compounds (Fig. 2) also display one weight loss step due to the removal of adsorbed water molecules. For the different forms of **1**, **2** and **3**, the observed weight losses are consistent with the calculated ones as well as the elemental analyses (Table 1 and Table S1, ESI†), indicating phase purity of the compounds.

The high thermal stability of the compounds has also been verified by temperature-dependent XRPD (TDXRPD) measurements. According to the TDXRPD patterns (Fig. S11–S13, ESI†), **1**, **2** and **3** are stable up to 220, 360 and 450 °C, respectively. It should be noted that the thermal stabilities obtained from the TDXRPD measurements (6 °C min^{-1}) can not be compared with those observed from TG analyses (2 °C min^{-1}) due to the employment of different heating rates in the two types of measurements.

In order to evaluate the chemical stabilities of the three functionalized UiO-66-X compounds, the samples were stirred in water, acetic acid, 1 M HCl and 1 M NaOH solutions for 12 h. Subsequently, the solids were collected by filtration and

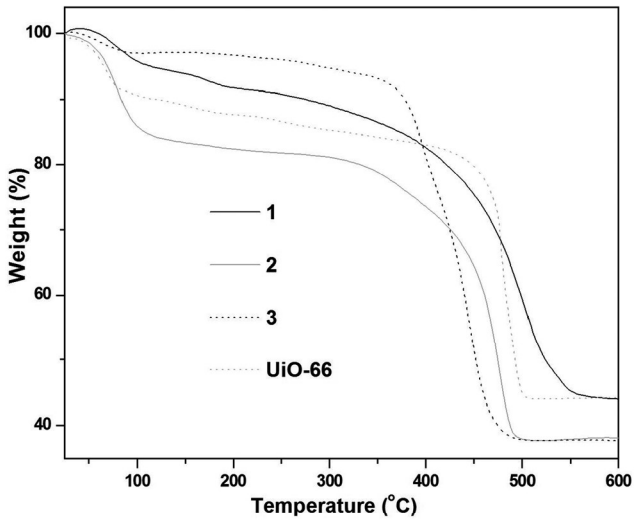

Fig. 2 TG curves of hydrated **1** (black, solid line), **2** (grey, solid line), **3** (black, dotted line) and UiO-66 (grey, dotted line) recorded in an air atmosphere in the temperature range 25–600 °C.

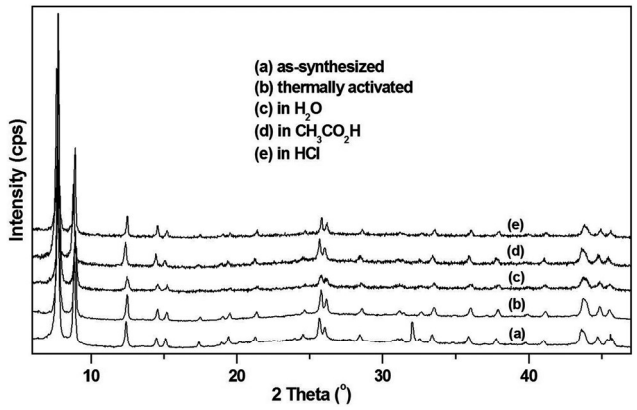

Fig. 3 XRPD patterns of **1** in different forms: as-synthesized (a), thermally activated (b), treated with water (c), acetic acid (d) and 1 M HCl (e).

characterized by XRPD analysis (Fig. 3 and Fig. S14–S15, ESI†). All of the three solids maintained their crystallinity after treatment with water, acetic acid and 1 M HCl solutions. However, all of them lost their crystallinity and became completely amorphous after treatment with 1 M NaOH solution. X-ray fluorescence analyses were carried out with the solutions obtained after filtration of the suspensions of the solids in 1 M HCl. No zirconium was detected in the solutions, which further corroborated the fact that the solids maintained their structural integrity in 1 M HCl. The chemical stabilities of the functionalized compounds are similar to those of unfunctionalized[36] and other functionalized UiO-66-X (X = –Br, $–NO_2$, $–NH_2$, $–(CH_3)_2$)[21,39] compounds.

Gas sorption properties

The N_2 sorption measurements performed on the thermally activated compounds reveal type-I adsorption isotherms for **2** and **3**, whereas a small sub-step is observed for **1** below

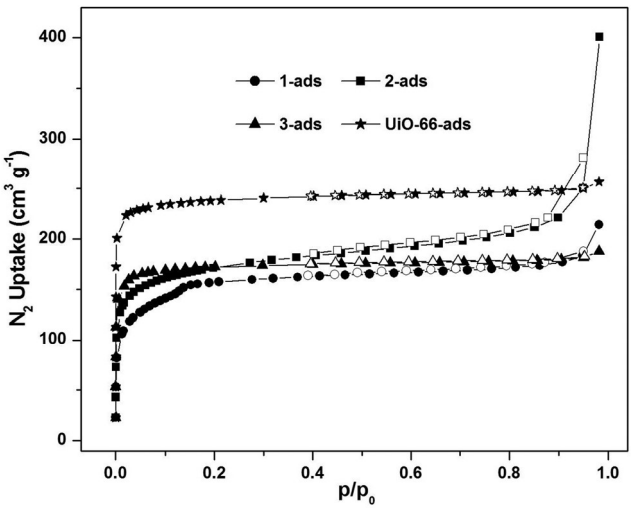

Fig. 4 Low pressure N_2 adsorption (closed symbols) and desorption (open symbols) isotherms of the thermally activated **1** (circles), **2** (squares), **3** (triangles) and UiO-66 (stars) recorded at –196 °C.

Table 3 Specific Langmuir surface areas and micropore volumes of the UiO-66-X compounds determined from N_2 adsorption isotherms

Compound	Specific Langmuir surface area[a] ($m^2\ g^{-1}$)	Micropore volume[b] ($cm^3\ g^{-1}$)
1	769	0.26
2	842	0.29
3	799	0.27
UiO-66	1086	0.38

[a] The specific Langmuir surface areas have been calculated from the N_2 adsorption isotherms. [b] The micropore volumes have been calculated at $p/p_0 = 0.5$.

p/p_0 = 0.2 (Fig. 4). The sub-step at p/p_0 = 0.13 that has been reproducibly observed in the N_2 adsorption isotherm of compound **1** can be tentatively assigned to the filling of two different types of cages (smaller tetrahedral and larger octahedral cages) present in the framework. The micropore volumes calculated from the N_2 adsorption isotherm of compound **1** at p/p_0 values of 0.13 (sub-step region) and 0.8 (saturation region) are 0.23 and 0.27 $cm^3\ g^{-1}$, respectively. The micropore volumes (Table 3) derived from the N_2 adsorption isotherms of all the compounds at p/p_0 = 0.5 exhibit considerable porosities, which are lower than the ones reported for unfunctionalized UiO-66.[36]

The high pressure CO_2 and CH_4 sorption isotherms (Fig. 5) measured on the thermally activated compounds at 33 °C show type-I isotherms. The CO_2 and CH_4 adsorption capacities of all the compounds at 33 °C and 25 bar are summarized in Table 4. The UiO-66-CO_2H compound shows the highest CO_2 uptake at 25 bar. The CO_2 adsorption capacity of **1** equals that of unmodified UiO-66 at 25 bar. The decreasing order of CO_2 uptake values at 25 bar is **2** > **1** = UiO-66 > **3**. As predicted in a previous report by computational methodology,[47] the introduction of polar functional groups such as $–CO_2H$ and $–SO_3H$ in

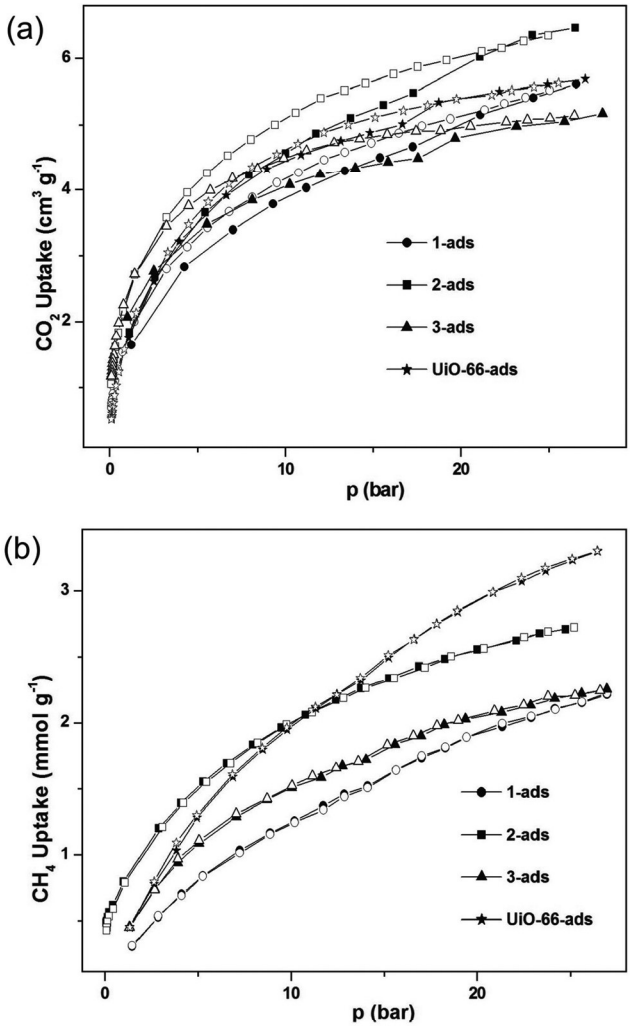

Fig. 5 High pressure (a) CO_2 and (b) CH_4 adsorption (closed symbols) and desorption (open symbols) isotherms of the thermally activated **1** (circles), **2** (squares), **3** (triangles) and UiO-66 (stars) measured at 33 °C.

Table 4 CO_2 and CH_4 uptake values at 25 bar as well as ideal CO_2/CH_4 adsorption selectivity of the UiO-66-X compounds at 33 °C

Compound	CO_2 uptake (mmol g^{-1})	CH_4 uptake (mmol g^{-1})	Ideal CO_2/CH_4 adsorption selectivity
1	5.6	2.1	4.5
2	6.4	2.7	5.2
3	5.1	2.2	4.7
UiO-66	5.6	3.2	2.6

the UiO-66 framework enhances the CO_2 uptake values, in spite of the lower specific Langmuir surface areas of the functionalized compounds compared to the unfunctionalized UiO-66. In sharp contrast to the CO_2 uptake sequence, the CH_4 adsorption capacity of the compounds decreases in the order UiO-66 > **2** > **3** > **1**. Interestingly, this CH_4 uptake sequence is similar to the order of the specific Langmuir surface area (Table 3) of the compounds. Thus, the CH_4 adsorption capacity of the functionalized compounds is governed by the pore dimensions, whereas the polarity of the functional groups plays a crucial role in determining the CO_2 uptake. From the initial slope of the single-component CO_2 and CH_4 adsorption isotherms, ideal CO_2/CH_4 selectivities (as ratios of the initial slopes) were determined.[68–70] The ideal CO_2/CH_4 adsorption selectivities (Table 4) of all the three compounds (4.5–5.2) were found to be higher compared to that of the parent UiO-66 compound (2.6). This selectivity trend is also in agreement with the previously predicted sequence of CO_2/CH_4 selectivity of the compounds.[47] It is noteworthy that similar or even higher CO_2/CH_4 selectivity values have formerly been achieved by a variety of MOFs.[68,71–77]

In the previous theoretical study,[47] the CO_2/CH_4 adsorption selectivities for their equimolar mixtures in the UiO-66-X compounds have been calculated as a function of the bulk pressure. On the other hand, the CO_2/CH_4 adsorption selectivities herein have been deduced as ratios of the initial slopes of the single-component CO_2 and CH_4 adsorption isotherms. Thus, only the trend (but not the absolute values) of CO_2/CH_4 adsorption selectivities observed in the present work can be compared with that of the previous theoretical report.

In order to determine the dynamic CO_2/CH_4 adsorption selectivities of the UiO-66-X compounds, breakthrough experiments have been performed using equimolar mixtures of the two gases at 298 K. The methods for the breakthrough experiments and the corresponding curves (Fig. S16, ESI†) are presented in the ESI.† The breakthrough profiles clearly reveal that the individual retention times of CO_2 and CH_4 for the functionalized UiO-66-X (X = $-SO_3H$, $-CO_2H$, –I) compounds are higher compared to those of the parent UiO-66 compound. However, under the present experimental conditions, we have been unable to achieve higher separation of CO_2 and CH_4 for the functionalized compounds compared to the unfunctionalized compounds.

Conclusions

The synthesis, characterization, stability and sorption analysis of three new functionalized UiO-66-X (X = $-SO_3H$, $-CO_2H$, –I) compounds have been demonstrated. The phase purity of the compounds was confirmed by a combination of XRPD analysis, DRIFT spectroscopy, thermogravimetric and elemental analysis. Thermogravimetric analyses show that **1**, **2** and **3** are stable up to 260, 340 and 360 °C, respectively. The high chemical stabilities of the compounds have been verified by XRPD analysis of the samples recovered after suspending them in water, acetic acid and 1 M HCl. The N_2, CO_2 and CH_4 sorption analyses exhibit significant microporosity for all the three compounds, which are comparable to the unfunctionalized UiO-66 compound, in spite of a large difference in specific surface areas between the functionalized and the unfunctionalized compounds. The CO_2 and CH_4 adsorption capacities of the compounds are governed by the polarity of the attached functional groups and the pore size, respectively. The ideal CO_2/CH_4 adsorption selectivities of all the three compounds,

measured from single component adsorption isotherms, are found to be higher compared to that of the pristine UiO-66 compound. The results obtained from single-component CO_2 and CH_4 adsorption isotherms verify the previous theoretical predictions,[47] thus establishing the potential of these functionalized compounds for the purification of biogas and landfill gas.

Acknowledgements

This research is funded by Ghent University, GOA grant number 01G00710.

Notes and references

1 K. Sumida, D. L. Rogow, J. A. Mason, T. M. McDonald, E. D. Bloch, Z. R. Herm, T.-H. Bae and J. R. Long, *Chem. Rev.*, 2012, **112**, 724.
2 G. Férey, *Chem. Soc. Rev.*, 2008, **37**, 191.
3 S. Kitagawa, R. Kitaura and S. Noro, *Angew. Chem.*, 2004, **116**, 2388, (*Angew. Chem., Int. Ed.*, 2004, **43**, 2334).
4 O. M. Yaghi, M. O'Keeffe, N. W. Ockwig, H. K. Chae, M. Eddaoudi and J. Kim, *Nature*, 2003, **423**, 705–714.
5 L. J. Murray, M. Dincă and J. R. Long, *Chem. Soc. Rev.*, 2009, **38**, 1294.
6 J.-R. Li, R. J. Kuppler and H.-C. Zhou, *Chem. Soc. Rev.*, 2009, **38**, 1477.
7 L. Hamon, P. L. Llewellyn, T. Devic, A. Ghoufi, G. Clet, V. Guillerm, G. D. Pirngruber, G. Maurin, C. Serre, G. Driver, W. van Beek, E. Jolimaitre, A. Vimont, M. Daturi and G. Férey, *J. Am. Chem. Soc.*, 2009, **131**, 17490.
8 J. Lee, O. K. Farha, J. Roberts, K. A. Scheidt, S. T. Nguyen and J. T. Hupp, *Chem. Soc. Rev.*, 2009, **38**, 1450.
9 L. Ma, C. Abney and W. Lin, *Chem. Soc. Rev.*, 2009, **38**, 1248.
10 K. M. L. Taylor-Pashow, J. Della Rocca, Z. G. Xie, S. Tran and W. B. Lin, *J. Am. Chem. Soc.*, 2009, **131**, 14261.
11 P. Horcajada, T. Chalati, C. Serre, B. Gillet, C. Sebrie, T. Baati, J. F. Eubank, D. Heurtaux, P. Clayette, C. Kreuz, J. S. Chang, Y. K. Hwang, V. Marsaud, Y.-N. Bories, L. Cynober, S. Gil, G. Férey, P. Couvreur and R. Gref, *Nat. Mater.*, 2010, **9**, 172.
12 M. Vallet-Regí, F. Balasm and D. Arcos, *Angew. Chem.*, 2007, **119**, 7692, (*Angew. Chem., Int. Ed.*, 2007, **46**, 7548).
13 P. Horcajada, C. Serre, M. Vallet-Regí, M. Sebban, F. Taulelle and G. Férey, *Angew. Chem.*, 2006, **118**, 6120, (*Angew. Chem., Int. Ed.*, 2006, **45**, 5974).
14 M. Eddaoudi, J. Kim, N. Rosi, D. Vodak, J. Wachter, M. O'Keefe and O. M. Yaghi, *Science*, 2002, **295**, 469.
15 C. Yang, X. P. Wang and M. A. Omary, *J. Am. Chem. Soc.*, 2007, **129**, 15454.
16 S. Horike, S. Bureekaew and S. Kitagawa, *Chem. Commun.*, 2008, 471.
17 S. T. Meek, J. J. Perry IV, S. L. Teich-McGoldrick, J. A. Greathouse and M. D. Allendorf, *Cryst. Growth Des.*, 2011, **11**, 4309.
18 F. Debatin, K. Behrens, J. Weber, I. A. Baburin, A. Thomas, J. Schmidt, I. Senkovska, S. Kaskel, A. Kelling, N. Hedin, Z. Bacsik, S. Leoni, G. Seifert, C. Jäger, C. Günter, U. Schilde, A. Friedrich and H.-J. Holdt, *Chem.–Eur. J.*, 2012, **18**, 11630.
19 R. Custelcean and M. G. Gorbunova, *J. Am. Chem. Soc.*, 2005, **127**, 16362.
20 V. Colombo, C. Montoro, A. Maspero, G. Palmisano, N. Masciocchi, S. Galli, E. Barea and J. A. R. Navarro, *J. Am. Chem. Soc.*, 2012, **134**, 12830.
21 M. Kandiah, M. H. Nilsen, S. Usseglio, S. Jakobsen, U. Olsbye, M. Tilset, C. Larabi, E. A. Quadrelli, F. Bonino and K. P. Lillerud, *Chem. Mater.*, 2010, **22**, 6632.
22 B. Wang, A. P. Cote, H. Furukawa, M. O'Keeffe and O. M. Yaghi, *Nature*, 2008, **453**, 207.
23 L. Hamon, E. Jolimaître and G. D. Pirngruber, *Ind. Eng. Chem. Res.*, 2010, **49**, 7497.
24 Y.-S. Bae, B. G. Hauser, O. M. Farha, J. T. Hupp and R. Q. Snurr, *Microporous Mesoporous Mater.*, 2011, **141**, 231.
25 S. Keskin, T. M. van Heest and D. S. Sholl, *ChemSusChem*, 2010, **3**, 879.
26 R. Babarao, S. Dai and J. Jiang, *Langmuir*, 2011, **27**, 3451.
27 Y. Zhao, H. Wu, T. J. Emge, Q. Gong, N. Nijem, Y. J. Chabal, L. Kong, D. C. Langreth, H. Liu, H. Zeng and J. Li, *Chem.–Eur. J.*, 2011, **17**, 5101.
28 A. Torrisi, R. G. Belland and C. Mellot-Draznieks, *Cryst. Growth Des.*, 2010, **10**, 2839.
29 W. Mu, D. Liu, Q. Yang and C. Zhong, *Microporous Mesoporous Mater.*, 2010, **130**, 76.
30 A. Demessence, D. M. D'Alessandro, M. L. Foo and J. R. Long, *J. Am. Chem. Soc.*, 2009, **131**, 8784.
31 L. M. Huang, H. T. Wang, J. X. Chen, Z. B. Wang, J. Y. Sun, D. Y. Zhao and Y. S. Yan, *Microporous Mesoporous Mater.*, 2003, **58**, 105.
32 J. A. Greathouse and M. D. Allendorf, *J. Am. Chem. Soc.*, 2006, **128**, 10678.
33 Y. Li and R. T. Yang, *Langmuir*, 2007, **23**, 12937.
34 S. S. Kaye, A. Dailly, O. M. Yaghi and J. R. Long, *J. Am. Chem. Soc.*, 2007, **129**, 14176.
35 D. Ma, Y. Li and Z. Li, *Chem. Commun.*, 2011, **47**, 7377.
36 J. H. Cavka, S. Jakobsen, U. Olsbye, N. Guillou, C. Lamberti, S. Bordiga and K. P. Lillerud, *J. Am. Chem. Soc.*, 2008, **130**, 13850.
37 Q. Yang, H. Jobic, F. Salles, D. Kolokolov, V. Guillerm, C. Serre and G. Maurin, *Chem.–Eur. J.*, 2011, **17**, 8882.
38 Q. Yang, A. D. Wiersum, H. Jobic, V. Guillerm, C. Serre, P. L. Llewellyn and G. Maurin, *J. Phys. Chem. C*, 2011, **115**, 13768, and references therein.
39 Y. Huang, W. Qin, Z. Li and Y. Li, *Dalton Trans.*, 2012, **41**, 9283.
40 M. Kim, S. J. Garibay and S. M. Cohen, *Inorg. Chem.*, 2011, **50**, 729.

41 C. Zlotea, D. Phanon, M. Mazaj, D. Heurtaux, V. Guillerm, C. Serre, P. Horcajada, T. Devic, E. Magnier, F. Cuevas, G. Férey, P. L. Llewellyn and M. Latroche, *Dalton Trans.*, 2011, **40**, 4879.

42 W. Morris, C. J. Doonan and O. M. Yaghi, *Inorg. Chem.*, 2011, **50**, 6853.

43 M. Kim, J. A. Boissonnault, P. V. Dau and S. M. Cohen, *Angew. Chem., Int. Ed.*, 2011, **50**, 12193.

44 M. L. Foo, S. Horike, T. Fukushima, Y. Hijikata, Y. Kubota, M. Takataf and S. Kitagawa, *Dalton Trans.*, 2012, **41**, 13791.

45 S. J. Garibay and S. M. Cohen, *Chem. Commun.*, 2010, **46**, 7700.

46 F. Vermoortele, M. Vandichel, B. Van de Voorde, R. Ameloot, M. Waroquier, V. Van Speybroeck and D. E. De Vos, *Angew. Chem., Int. Ed.*, 2012, **51**, 4887.

47 Q. Yang, A. D. Wiersum, P. L. Llewellyn, V. Guillerm, C. Serre and G. Maurin, *Chem. Commun.*, 2011, **47**, 9603.

48 S. T. Meek, J. J. Perry IV, S. L. Teich-McGoldrick, J. A. Greathouse and M. D. Allendorf, *Cryst. Growth Des.*, 2011, **11**, 4309.

49 V. Petricek, M. Dusek and L. Palatinus, *Jana2000, The Crystallographic Computing System*, Institute of Physics, Praha, Czech Republic, 2000.

50 P. S. Bárcia, D. Guimarães, P. A. P. Mendes, J. A. C. Silva, V. Guillerm, H. Chevreau, C. Serre and A. E. Rodrigues, *Microporous Mesoporous Mater.*, 2011, **139**, 67.

51 N. Stock and S. Biswas, *Chem. Rev.*, 2012, **112**, 933.

52 F. Vermoortele, R. Ameloot, A. Vimont, C. Serre and D. De Vos, *Chem. Commun.*, 2011, **47**, 1521.

53 C. Wang, Z. Xie, K. E. deKrafft and W. Lin, *J. Am. Chem. Soc.*, 2011, **133**, 13445.

54 A. Schaate, S. Dühnen, G. Platz, S. Lilienthal, A. M. Schneider and P. Behrens, *Eur. J. Inorg. Chem.*, 2012, 790.

55 V. Guillerm, F. Ragon, M. Dan-Hardi, T. Devic, M. Vishnuvarthan, B. Campo, A. Vimont, G. Clet, Q. Yang, G. Maurin, G. Férey, A. Vittadini, S. Gross and C. Serre, *Angew. Chem., Int. Ed.*, 2012, **51**, 9267.

56 A. Schaate, P. Roy, A. Godt, J. Lippke, F. Waltz, M. Wiebcke and P. Behrens, *Chem.–Eur. J.*, 2011, **17**, 6643.

57 C. Wang, K. E. deKrafft and W. Lin, *J. Am. Chem. Soc.*, 2012, **134**, 7211.

58 S. Chavan, J. G. Vitillo, D. Gianolio, O. Zavorotynska, B. Civalleri, S. Jakobsen, M. H. Nilsen, L. Valenzano, C. Lamberti, K. P. Lillerud and S. Bordiga, *Phys. Chem. Chem. Phys.*, 2012, **14**, 1614.

59 G. Wismann, A. Schaate, S. Lilienthal, I. Bremer, A. M. Schneider and P. Behrens, *Microporous Mesoporous Mater.*, 2012, **152**, 64.

60 A. Schaate, P. Roy, T. Preuße, S. J. Lohmeier, A. Godt and P. Behrens, *Chem.–Eur. J.*, 2011, **17**, 9320.

61 Q. Yang, V. Guillerm, F. Ragon, A. D. Wiersum, P. L. Llewellyn, C. Zhong, T. Devic, C. Serre and G. Maurin, *Chem. Commun.*, 2012, **48**, 9831.

62 A. D. Wiersum, E. Soubeyrand-Lenoir, Q. Yang, B. Moulin, V. Guillerm, M. B. Yahia, S. Bourrelly, A. Vimont, S. Miller, C. Vagner, M. Daturi, G. Clet, C. Serre, G. Maurin and P. L. Llewellyn, *Chem. Asian J.*, 2011, **6**, 3270.

63 W. Morris, B. Volosskiy, S. Demir, F. Gándara, P. L. McGrier, H. Furukawa, D. Cascio, J. F. Stoddart and O. M. Yaghi, *Inorg. Chem.*, 2012, **51**, 6443.

64 V. Bon, V. Senkovskyy, I. Senkovska and S. Kaskel, *Chem. Commun.*, 2012, **48**, 8407.

65 S. Biswas, T. Ahnfeldt and N. Stock, *Inorg. Chem.*, 2011, **50**, 9518.

66 M. G. Goesten, J. Juan-Alcañiz, E. V. Ramos-Fernandez, K. B. S. S. Gupta, E. Stavitski, H. van Bekkum, J. Gascon and F. Kapteijn, *J. Catal.*, 2011, **281**, 177.

67 V. Guillerm, S. Gross, C. Serre, T. Devic, M. Bauer and G. Férey, *Chem. Commun.*, 2010, **46**, 767.

68 R. Banerjee, H. Furukawa, D. Britt, C. Knobler, M. O'Keeffe and O. M. Yaghi, *J. Am. Chem. Soc.*, 2009, **131**, 3875.

69 J. An, S. J. Geib and N. L. Rosi, *J. Am. Chem. Soc.*, 2010, **132**, 38.

70 X. Si, C. Jiao, F. Li, J. Zhang, S. Wang, S. Liu, Z. Li, L. Sun, F. Xu, Z. Gabelica and C. Schick, *Energy Environ. Sci.*, 2011, **4**, 4522.

71 B. Zheng, Z. Yang, J. Bai, Y. Li and S. Li, *Chem. Commun.*, 2012, **48**, 7025.

72 J. Duan, Z. Yang, J. Bai, B. Zheng, Y. Li and S. Li, *Chem. Commun.*, 2012, **48**, 3058.

73 Y.-S. Bae, O. K. Farha, A. M. Spokoyny, C. A. Mirkin, J. T. Hupp and R. Q. Snurr, *Chem. Commun.*, 2008, 4135.

74 J. Ferrando-Soria, P. Serra-Crespo, M. de Lange, J. Gascon, F. Kapteijn, M. Julve, J. Cano, F. Lloret, J. Pasán, C. Ruiz-Pérez, Y. Journaux and E. Pardo, *J. Am. Chem. Soc.*, 2012, **134**, 15301.

75 V. Finsy, L. Maa, L. Alaerts, D. E. De Vos, G. V. Baron and J. F. M. Denayer, *Microporous Mesoporous Mater.*, 2009, **120**, 221.

76 S. Couck, J. F. M. Denayer, G. V. Baron, T. Rémy, J. Gascon and F. Kapteijn, *J. Am. Chem. Soc.*, 2009, **131**, 6326.

77 L. Hamon, N. Heymans, P. L. Llewellyn, V. Guillerm, A. Ghoufi, S. Vaesen, G. Maurin, C. Serre, G. De Weireld and G. D. Pirngruber, *Dalton Trans.*, 2012, **41**, 4052.